Int J Thermophys (2009) 30:608–618
DOI 10.1007/s10765-008-0525-7

Improvements in the Dynamic Plane Source Method

Svetozár Malinarič · Peter Dieška

Received: 31 March 2008 / Accepted: 13 October 2008 / Published online: 11 November 2008

Abstract Three sources of errors in the extended dynamic plane source (EDPS) method caused by the discrepancy between experiment and model are analyzed. The source effect is eliminated by introducing the nuisance parameter R_0 and the surface effect by a surrounding vacuum. The original model assumes a constant heating power but a constant current is used in the experiment. Suppression of this effect leads to a new solution of the heat equation designated as the constant-current model. The measurements on polymethylmetacrylate (PMMA) in vacuum, evaluated by the constant-current model, provided results of $\lambda = 0.191\ \mathrm{W{\cdot}m^{-1}{\cdot}K^{-1}}$ and $a = 0.118 \times 10^{-6}\ \mathrm{m^2{\cdot}s^{-1}}$, which are in good agreement with published values. The total standard uncertainty was estimated as 1.5 % for both thermophysical properties.

Keywords Constant-current model · Difference analysis · Polymethylmetacrylate · Thermal conductivity · Thermal diffusivity · Transient method

1 Introduction

Dynamic methods [1] for measurements of thermophysical properties can be divided into contact (transient) and non-contact (flash) methods. The former are based on generation of a dynamic temperature field inside the specimen. This experimental arrangement suppresses the sample surface influence on the measuring process.

S. Malinarič (✉)
Department of Physics, Constantine the Philosopher University, Trieda Andreja Hlinku 1, 94974 Nitra, Slovak Republic
e-mail: smalinaric@ukf.sk

P. Dieška
Department of Physics, Faculty of Electrical Engineering and Informatics, Slovak University of Technology, Ilkovičova 3, 81219 Bratislava, Slovak Republic

Transient methods use both a two-probe system (heat source and thermometer are separated) and one-probe system (heat source and thermometer are the same).

The dynamic plane source (DPS) method [2] is arranged for one-dimensional heat flow into a finite sample. The rear sides of the samples are in contact with a poor thermal conducting material so that the temperature developed in the sample is close to adiabatic. This method appears to be useful for simultaneous determination of the thermal conductivity and thermal diffusivity in metals.

The extended dynamic plane source (EDPS) method [3] is a modification of the DPS method for materials with a thermal conductivity $\lambda < 2\ \mathrm{W \cdot m^{-1} \cdot K^{-1}}$. The heat source, which simultaneously serves as the thermometer, is placed between two identical specimens. The heat sink, made of a very good thermal conducting material, provides isothermal boundary conditions for the experiment. Heat is produced by the passage of an electrical current in the form of a stepwise function with time through the planar electrical resistance—heat source. The thermal conductivity λ and thermal diffusivity a of the specimen can be calculated from the temperature response.

A theoretical model of the experiment is described by the heat equation. The temperature function is a solution of this equation with boundary and initial conditions corresponding to the experimental arrangement. The principle of the method consists of fitting the temperature function to the experimental points (temperature response).

The measurement error consists of the following components:

1. Ideal model errors are caused by deviations of the experimental arrangement from the theoretical model.
   (a) Source effect—the model assumes a homogenous heat source with negligible heat capacity and ideal thermal contact with a specimen.
   (b) Surface effect—the model assumes no heat losses from the lateral sides of the specimen and heat source.
   (c) Current effect—the model also assumes a constant power, but in the experiment, a constant current is used.
2. Random errors are caused by electronic noise, fitting procedure, variation in temperature, apparatus assembly, and other unknown variations in the timescale of measurement. The associated uncertainty can be determined based on the measurement repeatability.
3. Measurement errors are caused by input parameter measurements. Their associated uncertainties are combined according to the rules defined by GUM [4].

The aim of this work is to analyze the ideal model errors and improve the EDPS method.

2 Constant-Power Model

The original model presented by Karawacki [2,3] applied the following conditions:

(i) The heat flow is one-dimensional, and the heat source and specimens are infinite, parallel slabs.
(ii) The heat source is homogenous with negligible thickness and heat capacity.
(iii) There is no thermal resistance between the heat source and specimen.

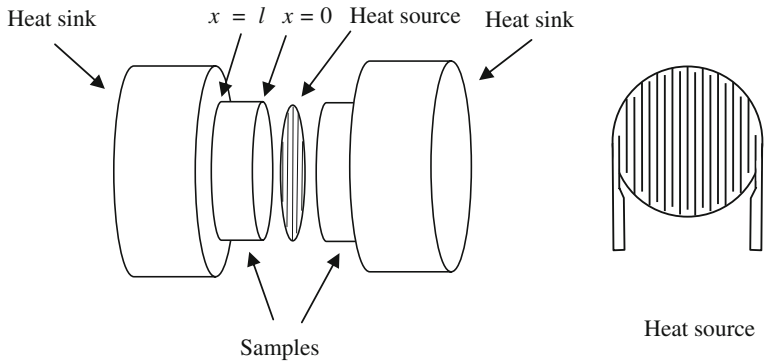

Fig. 1 Setup of the EDPS experiment

(iv) The heat sink is semi-infinite with known thermal properties.
(v) There is ideal thermal contact between the specimen and heat sink.
(vi) The input heat power is constant.

In order to eliminate the source effect, we changed the 3rd condition in the model to:

(iii) There is a constant contact thermal resistance between the heat source and specimen.

The experimental arrangement of the EDPS method is shown in Fig. 1. Before the start of the experiment, the temperature of the specimen, heat source, and heat sink is stabilized and is equal to T_0. A short time Θ_h after the start, a steady state at the boundary between the heat source and specimen is reached and Newton's cooling law can be written as [5]

$$q = h(T_\mathrm{h} - T|_{x=0}), \tag{1}$$

where q is the heat current density, h is the heat transfer coefficient, and T_h is the temperature increase of the heat source. The temperature difference is caused not only by the thermal contact between the specimen and heat source but also by its meander-like shape.

Then the temperature of the heat source can be expressed as

$$T_\mathrm{H}(t) = T_0 + T_\mathrm{h}(t) = T_0 + \frac{q}{h} + T|_{x=0}\,, \tag{2}$$

and the temperature increase of the specimen in the plane for $x = 0$ (temperature function) is given by [3]

$$T|_{x=0} = \frac{F(t,a)}{\lambda}, \tag{3}$$

where

$$F(t,a) = q\sqrt{\frac{at}{\pi}}\left(1 + 2\sqrt{\pi}\sum_{n=1}^{\infty}\beta^n \text{ierfc}\left(\frac{nl}{\sqrt{at}}\right)\right), \tag{4}$$

l is the thickness of the specimen and ierfc is the error function integral [6]. Parameter β describes the heat sink imperfection and is given by

$$\beta = \left(\lambda/\sqrt{a} - \lambda_s/\sqrt{a_s}\right) / \left(\lambda/\sqrt{a} + \lambda_s/\sqrt{a_s}\right) \tag{5}$$

where λ_s is the thermal conductivity and a_s is the thermal diffusivity of the heat sink. The heat source temperature can be converted to resistance by the following formula:

$$R = R_0\left(1 + \alpha T\right), \tag{6}$$

where R_0 is the resistance at temperature $T = 0$ and α is the temperature coefficient of the heat source resistivity. Then the predicted values of the heat source resistance can be determined using Eqs. 3 and 6 as

$$r\left(t\right) = R_0\left(1 + \frac{\alpha}{\lambda}F\left(t,a\right)\right). \tag{7}$$

Two thermophysical parameters λ and a and one nuisance parameter R_0 should be iterated until the sum of $(r(t_i) - r_i)^2$ reaches its minimum, where $[t_i, r_i]$ are measured points. The sensitivity coefficients were analyzed in [7,8]. The Levenberg–Marquardt method [9] was used for sum-of-squares minimization.

Equation 2 is valid only for $t > \Theta_h$, which denotes the characteristic time of the heat source. The unknown value Θ_h can be determined using "difference analysis" [7,8] which is based on fitting in the time interval $(t_B, t_B + t_S)$. When t_B is successively increased while t_S is constant, the results of fitting λ and a can be plotted against t_B. We assume that the time interval is optimal when the results of fitting are not sensitive to changes of the interval, which causes the plots to have a plateau. So Θ_h will be estimated as the time at the beginning of the plateau.

3 Constant-Current Model

In order to eliminate the current effect, we define a new model, changing the 6th condition:

(vi) The time dependence of the heat power is known from the experiment.

The one-dimensional heat equations are

$$\frac{1}{a}\frac{\partial T}{\partial t} = \frac{\partial^2 T}{\partial x^2} \qquad 0 < x < l, \tag{8}$$

$$\frac{1}{a_s}\frac{\partial T}{\partial t} = \frac{\partial^2 T}{\partial x^2} \qquad l < x, \tag{9}$$

where T is the increase of the specimen temperature, so the initial condition is

$$T|_{t=0} = 0. \tag{10}$$

The boundary conditions are

$$T|_{x\to\infty} = 0, \tag{11}$$

$$T|_{x=l^-} = T|_{x=l^+}, \tag{12}$$

$$-\lambda \left.\frac{\partial T}{\partial x}\right|_{x=l^-} = -\lambda_s \left.\frac{\partial T}{\partial x}\right|_{x=l^+}, \tag{13}$$

$$-\lambda \left.\frac{\partial T}{\partial x}\right|_{x=0} = h\left(T_h - T|_{x=0}\right), \tag{14}$$

and the heat balance equation for the heat source is given by Eq. 1. Applying the Laplace transform [6], the increase of the heat source temperature will be given as the convolution,

$$T_h(t) = \int_0^t q(t-\tau)\, T_{Dir}(\tau)\, d\tau \tag{15}$$

where the temperature response to Dirac's pulse power input is

$$T_{Dir}(t) = \frac{\delta(t)}{h} + \frac{1}{\lambda}\sqrt{\frac{a}{\pi\, t}}\left(1 + 2\sum_{n=1}^{\infty}\beta^n e^{-\frac{l^2n^2}{at}}\right). \tag{16}$$

For the purpose of numerical evaluation, we express the temperature function in the form,

$$T_h(t_i) = \frac{q(t_i)}{h} + \frac{G(t_i, a)}{\lambda}, \tag{17}$$

where

$$G(t_i, a) = \Delta t\sqrt{\frac{a}{\pi}}\sum_{j=1}^{i}\frac{q\left(t_i - t_j\right)}{\sqrt{t_j}}\left(1 + 2\sum_{n=1}^{\infty}\beta^n e^{-\frac{l^2n^2}{at_j}}\right), \tag{18}$$

q is computed from the measured heat source resistivity response $[t_i, r_i]$ and $\Delta t = t_{i+1} - t_i$ for equispaced sampling. As the temperature difference between the heat source and specimen surface is small and the change of the heat current density during the experiment is also small, we can consider the first term in Eq. 17 to be constant. Then the predicted values of the heat source resistance can be determined using Eqs. 6 and 17,

$$r(t_i) = R_0\left(1 + \frac{\alpha}{\lambda}G(t_i, a)\right), \tag{19}$$

and fitted to measured points $[t_i, r_i]$ as described in Sect. 2. Since the function G is a corrected version of the function F and the parameters are the same, the sensitivity coefficients will be similar and the fitting will be successful.

4 Experiment

The heat source is fabricated from nickel foil 20 µm thick covered on both sides with a 25 µm Kapton layer. The diameter of the heat source is 30 mm, the electrical resistance is about 1 Ω, and the temperature coefficient of resistivity is $0.0047\,\mathrm{K}^{-1}$. The time dependence of the heat source resistance was recorded by means of an electrical circuit as shown in Fig. 2. The electrical current and the voltage across the heat source were measured using a constant-power resistor ($R_1 = 1\ \Omega$) and a multichannel computer plug-in card (PCL 816, Advantech). The electrical noise was suppressed by capacitors and numerical averaging.

The measurements were performed on PMMA (polymethylmetacrylate) samples, 30 mm in diameter and 2.97 mm in thickness. The electrical current in the heat source was set to values from 0.2 A to 0.8 A. Each temperature response was recorded for 300 points corresponding to 100 s at a temperature of 23 °C. The measurements were made in air and in vacuum of approximately 10 Pa. The thermal contact between the individual parts of the specimen set was improved by silicon oil.

5 Results and Discussion

Figures 3, 4, 5, and 6 illustrate the evaluation of the measurements made in vacuum with a heating current of 0.4 A using a constant-power model, Eq. 7. The difference analysis results are shown in Fig. 3, where the characteristic time of the heat source is estimated as $\Theta_\mathrm{h} \approx 10\,\mathrm{s}$ to 15 s. Estimates of the parameters can be determined from plateaus or by standard analysis [10,11] as shown in Fig. 4. The first 15 s are disregarded, and the size of the interval is successively increased. The results are more stable, and parameter estimates can easily be obtained.

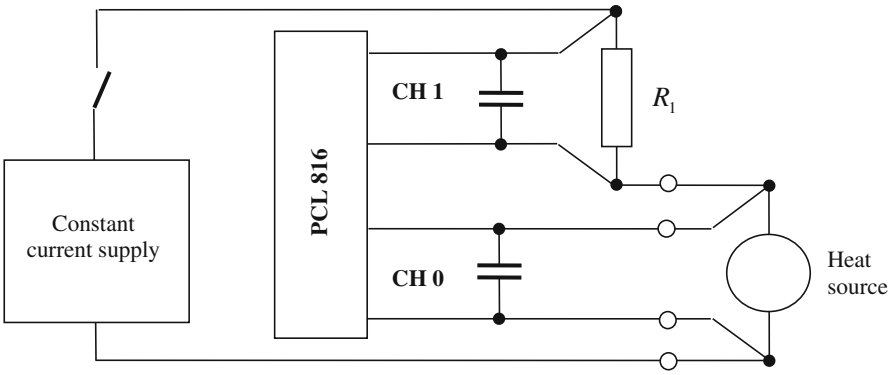

Fig. 2 Experimental circuit diagram

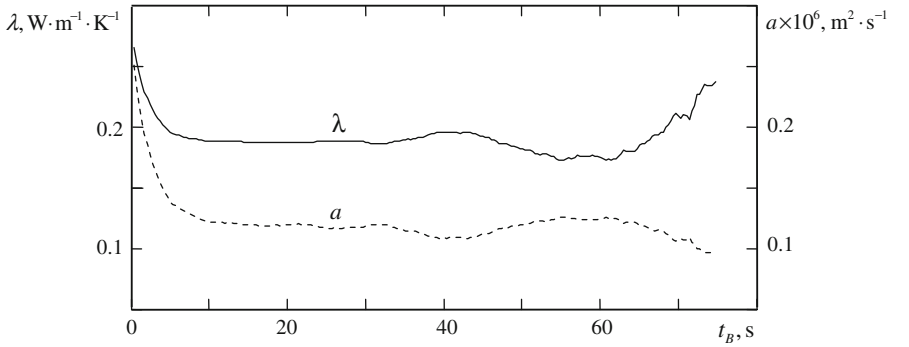

Fig. 3 Difference analysis—thermal conductivity λ and diffusivity a as a function of the time window $(t_B, t_B + t_S)$, $t_S = 25$ s

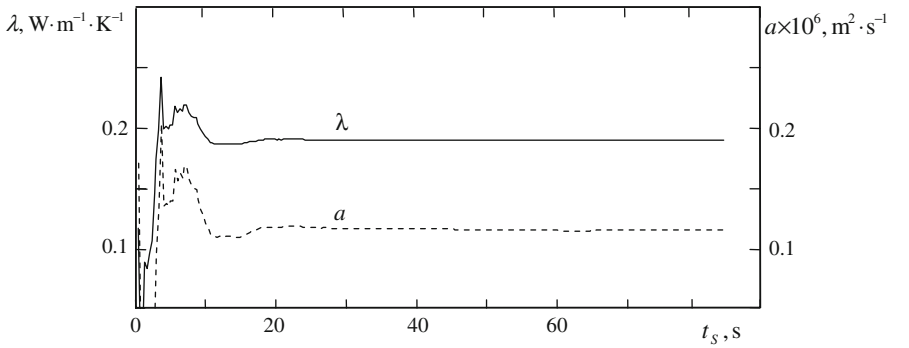

Fig. 4 Standard analysis—thermal conductivity λ and diffusivity a as a function of the time window $(t_B, t_B + t_S)$, $t_B = 15$ s

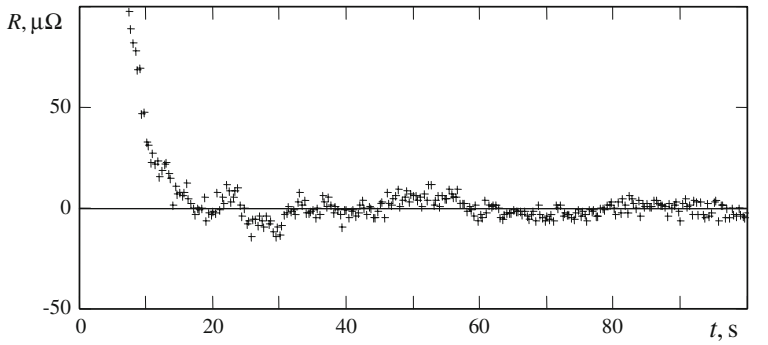

Fig. 5 Time dependence of residuals

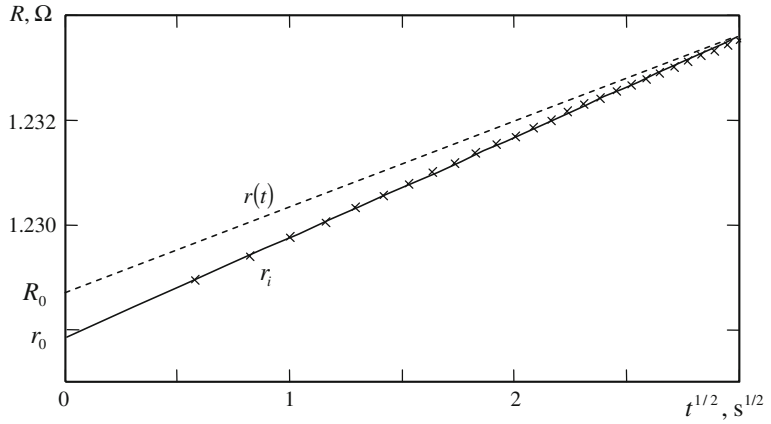

Fig. 6 Predicted $r(t)$ and measured r_i values at the start of the experiment

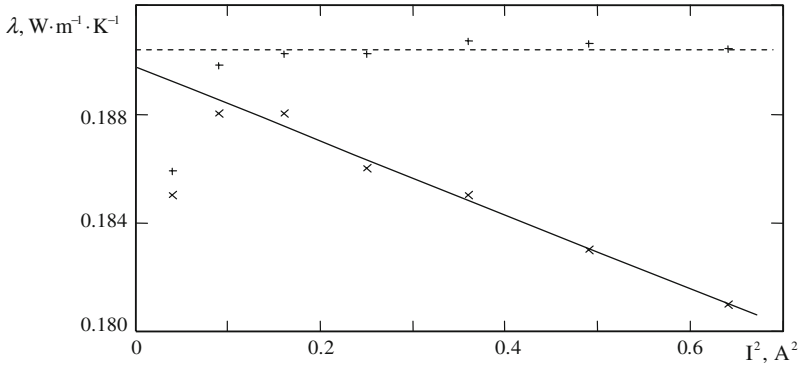

Fig. 7 Thermal conductivity computed by the constant-current (+) and constant-power (×) models

Once we have the thermophysical parameter estimates, we can verify the fitting procedure and estimation of Θ_h by plotting residuals [12] against time as shown in Fig. 5. The random component of the resistance measurement uncertainty (noise) can be evaluated from the variance of the residuals $u(R) = 5\,\mu\Omega$ corresponding to a heat source temperature of 1 mK. Figure 6 shows the discrepancy between the model $r(t)$ and measurements r_i for times less then 10 s. The difference between the extrapolated values $R_0 - r_0 = 0.79$ mΩ corresponds to a temperature difference between the heat source and specimen of 0.14 K in Eq. 1.

The surface effect was investigated by measurements in air (∼100 kPa) and in vacuum (∼10 Pa). The measurement with a heating current of 0.4 A was repeated five times and evaluated as described above. The instrument and specimens were disassembled and reassembled before each measurement. Table 1 presents a statistical evaluation of the measurement of the thermophysical parameters, where $s(\bar{x})$ is the experimental standard deviation of the mean $\bar{x}$. We used the standard t-test [13] at a significance level of 0.05 to demonstrate that heat losses into air influence the thermal conductivity but not the thermal diffusivity measurement. The standard uncertainty

Table 1 Comparison of the measurements on PMMA in air and in vacuum

Surrounding	$\frac{\bar{\lambda}}{(\mathrm{W{\cdot}m^{-1}{\cdot}K^{-1}})}$	$\frac{s(\bar{\lambda})}{(\mathrm{W{\cdot}m^{-1}{\cdot}K^{-1}})}$	$\frac{\bar{a}\times 10^6}{(\mathrm{m^2{\cdot}s^{-1}})}$	$\frac{s(\bar{a})\times 10^6}{(\mathrm{m^2{\cdot}s^{-1}})}$
Air	0.195	0.0018	0.120	0.0015
Vacuum	0.187	0.0023	0.118	0.0015

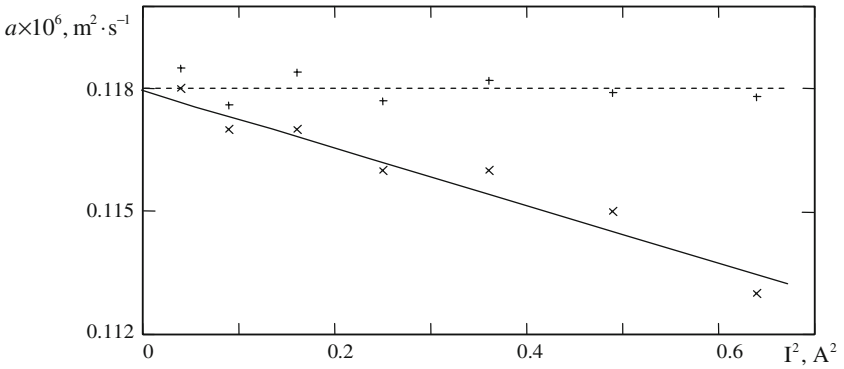

Fig. 8 Thermal diffusivity computed by the constant-current (+) and constant-power (×) models

associated with the measurement repeatability was estimated to be less then 1 % for all results presented in Table 1.

The current effect was studied by comparing the results of evaluation from the constant-power model of Eq. 7 to the results of the constant-current model, Eq. 19. Figures 7 and 8 show estimates of the thermophysical parameters as a function of the heating current, measured in vacuum. When a constant-power model is used, both thermophysical parameters, λ and a, show a strong dependence on the heating current. On the contrary, the results obtained using the constant-current model are stable and independent of the heating current. This shows that the latter model describes the experiment better. In addition, the results of both models correspond very well for low values of the heating current. Here it should be mentioned that a small heating current causes a small temperature change and consequently a large error in the estimation of the thermophysical parameters [11]. So the optimal heating current range, where the results of both models agree the best, is from 0.3 A to 0.4 A. This can also be demonstrated by a plot of the relative differences (Fig. 9), defined by the formula,

$$\frac{\Delta x}{x} = \frac{x_\mathrm{C} - x_\mathrm{P}}{x_\mathrm{C}}, \tag{20}$$

where x_C and x_P are the parameter values computed by the constant-current and constant-power models, respectively.

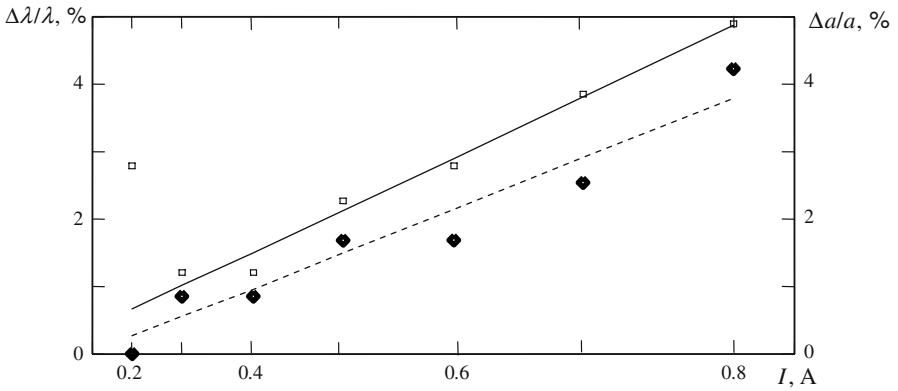

Fig. 9 Relative differences of the parameters λ(□) and a (•) versus the heating current

6 Summary

Three effects and two models of the EDPS method were analyzed and applied to measurements performed with a constant current. The source effect was solved using a constant-power model which resulted in fitting three parameters. One of the parameters R_0 corresponds to a temperature drop on the thermal contact resistance. The fitting gave very small residual variances for times larger than the characteristic time of the heat source Θ_h.

The surface effect was eliminated by a surrounding vacuum, which caused a decrease of about 4 % in thermal conductivity but a negligible change in the thermal diffusivity. This can be explained by heat losses from the lateral sides of the specimen and heat source.

The current effect was minimized using a constant-current model corresponding to the real experimental arrangement. We came to the conclusion that application of the constant-power model for measurements with a current of 0.3 A or 0.4 A can cause an error of about 1 %. The better solution is to measure with several values of the heating current and make the extrapolation to zero power, as seen in Fig. 9.

Measurements on PMMA in vacuum were evaluated using the constant-current model and provided results of $\lambda = 0.191\ \mathrm{W\cdot m^{-1}\cdot K^{-1}}$ and $a = 0.118\times10^{-6}\ \mathrm{m^2\cdot s^{-1}}$, which are in good agreement with published values [14], although the materials were not exactly identical. Considering the improvements presented here and the uncertainty assessment in [7], we can estimate the total standard uncertainty at 1.5 % for both thermophysical properties.

We can conclude that the described method can be safely used for materials with thermal conductivities in the range from $0.1\ \mathrm{W\cdot m^{-1}\cdot K^{-1}}$ to $2\ \mathrm{W\cdot m^{-1}\cdot K^{-1}}$. Materials with lower values of thermal conductivity will need a more in-depth analysis of heat losses, and materials with higher values should be measured with the DPS method.

Acknowledgment The authors wish to thank the Slovak Science Grant Agency for financial support under Contract 1/3178/06.

References

1. L'. Kubičár, V. Boháč, in *Proceedings of 24th Int. Conf. on Thermal Conductivity/12th Int. Thermal Expansion Symp.*, ed. by P.S. Gaal, D.E. Apostolescu (Technomic Pub., Lancaster, Pennsylvania, 1999), p. 135
2. E. Karawacki, B.M. Suleiman, Meas. Sci. Technol. **2**, 744 (1991)
3. E. Karawacki, B.M. Suleiman, I. ul-Haq, B. Nhi, Rev. Sci. Instrum. **63**, 4390 (1992)
4. *Guide to the Expression of the Uncertainty in Measurement* (ISO, Geneva, 1993)
5. S.E. Gustafsson, E. Karawacki, M.A. Chohan, J. Phys. D: Appl. Phys. **19**, 727 (1986)
6. H.S. Carslaw, J. Jaeger, *Conduction of Heat in Solids* (Clarendon, Oxford, 1959)
7. S. Malinarič, Meas. Sci. Technol. **15**, 807 (2004)
8. S. Malinarič, Int. J. Thermophys. **25**, 1913 (2004)
9. W.H. Press, S.A. Teukolsky, W.T. Vetterling, B.P. Flannery, *Numerical Recipes in C: The Art of Scientific Computing* (Cambridge University Press, Cambridge, 1994)
10. V. Boháč, M.K. Gustavsson, L'. Kubičár, S.E. Gustafsson, Rev. Sci. Instrum. **71**, 2452 (2000)
11. S. Malinarič, Int. J. Thermophys. **28**, 20 (2007)
12. J.V. Beck, K.J. Arnold, *Parameter Estimation in Engineering and Science* (Wiley, New York, 1977)
13. F. Lamoš, R. Potocký, *Pravdepodobnosť a matematická štatistika* (Alfa, Bratislava, 1989)
14. L'. Kubičár, V. Boháč, *Proc. Thermophys. 2002* (CPU, Nitra, 2002), p. 39